Physics of the Dark Universe 27 (2020) 100430

Contents lists available at ScienceDirect

Physics of the Dark Universe

journal homepage: www.elsevier.com/locate/dark

Connecting particle physics and cosmology: Measuring the dark matter relic density in compressed supersymmetry models at the LHC

Carlos Ávila [b], Andrés Flórez [b,*], Alfredo Gurrola [a], Dale Julson [a], Savanna Starko [a]

[a] Department of Physics and Astronomy, Vanderbilt University, Nashville, TN, 37235, USA
[b] Physics Department, Universidad de los Andes, Bogotá, Colombia

ARTICLE INFO

Article history:
Received 3 September 2019
Received in revised form 15 November 2019
Accepted 9 December 2019

ABSTRACT

The identity of Dark Matter (DM) is one of the relevant topics in particle physics today. The R-parity conserving Minimal Supersymmetric Standard Model (MSSM), which naturally provides a DM candidate in the form of the lightest neutralino ($\tilde{\chi}_1^0$), is used as a benchmark scenario to show that a measurement of the DM relic density, $\Omega_{\tilde{\chi}_1^0}h^2$, can be achieved from measurements at the CERN Large Hadron Collider. Focus is placed on compressed mass spectra regions, where the mass difference Δm between the $\tilde{\chi}_1^0$ and the supersymmetric partner of the tau lepton ($\tilde{\tau}_1$) is small and where the $\tilde{\tau}_1$-$\tilde{\chi}_1^0$ coannihilation (CA) mechanism of the early Universe plays an important role. The technique for measuring $\Omega_{\tilde{\chi}_1^0}h^2$ relies on two proposed searches for compressed Supersymmetry (SUSY): (1) production via Vector Boson Fusion (VBF) processes; and (2) production with associated energetic jets from initial state radiation (ISR). These approaches allow for the determination of the relic abundance at the LHC for any model where CA is an important DM reduction mechanism in the early Universe. Thus, it is possible to confirm that the DM we observe today corresponds to $\tilde{\chi}_1^0$'s created in the early Universe. We show that from measurements in the VBF and ISR SUSY searches at the LHC, the mass gap Δm and the dark matter relic density can be measured with an uncertainty of 4.5% and 25%, respectively, assuming 13 TeV proton–proton data from the high-luminosity LHC. The precise measurement of a small Δm value would also confirm the existence of $\tilde{\tau}_1$-$\tilde{\chi}_1^0$ CA.

1. Introduction

One of the important discoveries in modern cosmology is that the observable matter is only a small fraction of the total energy density of the Universe [1]. Only 5% of the Universe's energy density is "normal matter", 27% is Dark Matter (DM), and 68% is Dark Energy [2]. While there is evidence for DM revealed through gravitational interactions at macroscopic scales [3], the particle nature of DM remains unknown and constitutes an important question in science. If we could comprehend the nature of DM, we would make great progress in understanding the evolution of the Universe and its composition.

Hadron colliders have proven to be successful experimental tools to understand the smallest building blocks and fundamental forces. As proof, the ATLAS [4] and CMS [5] experiments at the CERN Large Hadron Collider (LHC) discovered the Higgs boson [6,7], which is the quantum of the Higgs field responsible for the generation of particle masses. Besides the study of the Higgs boson properties, the LHC has a broad research program that includes DM searches. Until now, searching for the identity of DM has proven to be difficult due to its unknown mass and possibly weakly interacting nature. In this latter case, it would be produced in hadron colliders at significantly lower rates than known processes mediated by the strong force producing similar detector signatures. Depending on the model, the range of possible DM mass values is also broad. In scenarios such as axion DM [8] or anapole DM [9], the mass values can be as low as 100 MeV and potentially beyond the reach of the LHC experiments. On the other hand, a weakly interacting massive particle (WIMP), such as the lightest neutralino in Supersymmetry (SUSY) [10–15], can be heavy enough to be found at the LHC, or have a mass value that exceeds the current energy frontier.

Since no positive sign of DM has been found yet at the LHC, it is possible that the only way to detect DM at a hadron collider is to target rare production mechanisms that, although giving low production rates, result in a very distinctive signature so that it could be identified amongst more abundantly produced processes. For example, the tagging of events using a Vector Boson Fusion (VBF) topology [16–24] or a highly energetic jet from initial state radiation (ISR) [25–29], have been proposed as two powerful experimental handles to discover the DM particle and other beyond standard model physics at the LHC [30–32].

* Corresponding author.
E-mail address: ca.florez@uniandes.edu.co (A. Flórez).

https://doi.org/10.1016/j.dark.2019.100430
2212-6864/

VBF tagging is effective at suppressing backgrounds from QCD processes dominating at a hadron collider. The use of a high p_T ISR jet boosts the detection of DM particles due to its recoiling effect. However, even if a hypothetical particle X is discovered at the LHC through the VBF and/or ISR mechanisms, it is not sufficient to claim X as the DM particle until its relic density is shown to be consistent with the one measured by astronomers. On the other hand, if X is discovered with the VBF/ISR analyses and the deduced relic density is not consistent with measurements from astronomy, this does not necessarily mean X is not the DM particle. It could mean our assumptions of the evolution of the Universe (Big Bang Cosmology) might not be correct (e.g. thermal vs non-thermal cosmology). In either case, a discovery at the LHC with the VBF/ISR DM analyses *and the subsequent determination of its relic density* has the potential to paint a more comprehensive picture of the DM particle interactions which existed in the early Universe and led to its current structure.

One current assumption is that at the inception of the Universe, DM particles could have been created and destroyed concurrently. Temperatures were high enough such that Standard Model (SM) particles had enough thermal kinetic energy to interact, annihilate, and produce DM [33]. Additionally, prior to the Universe's inflation, the concentration of DM was high enough that the DM particle content could be reduced, as DM particles underwent interactions producing SM or other beyond SM particles. As time progressed, the Universe expanded in the inflationary period, reducing temperatures in the process. The rate of DM creation diminished to practically zero as SM particles lost kinetic energy. In the expanded Universe, DM concentration became more diffuse, reducing the rate of DM annihilation. Since that critical time, the DM density has remained relatively constant [33], with a measured value of $\Omega_{\rm DM}h^2 \approx 0.120 \pm 0.001$ [2], and usually referred to as the DM relic density. However, in some physics models, particularly SUSY, $SM + SM \leftrightarrow DM + DM$ interactions are not sufficient to give way to the measured value. In some cases, a model of coannihilation (CA) is necessary to maintain consistency between particle physics and cosmology [34]. According to CA theory, the DM particle has a CA partner Υ, yet to be discovered, which interacts with the DM particle in the early Universe and coannihilates to produce SM particles, reducing the DM content in a way consistent with current cosmological measurements from the Wilkinson Microwave Anisotropy Probe (WMAP) [1] and Planck collaborations [2]. Since the CA cross-section depends exponentially on the mass splitting Δm between DM and Υ, $\langle\sigma v\rangle_{\rm CA} \sim e^{-\Delta m/T}$, the CA mechanism of the early Universe becomes important for DM physics in models with compressed mass spectra [35]. These compressed mass spectra regions are hallmark scenarios for the aforementioned VBF and ISR DM search methods at the LHC.

In this letter we propose a series of measurements at the LHC, using the VBF and ISR search channels to target a specific compressed physics phase space, to determine the role of CA, deduce the masses of relevant particles, and establish a prediction of $\Omega_{\rm DM}h^2$. A strong candidate for DM is the lightest neutralino ($\widetilde{\chi}_1^0$) in the R-parity conserving Minimal Supersymmetric Standard Model (MSSM). The lightest neutralino is a linear combination of Higgsino, Bino, and Wino — the SUSY partners of the SM gauge bosons [15]. In our benchmark scenario we assume $\widetilde{\chi}_1^0$ has a large Bino component, since this is the SUSY phase space where CA plays an important role. We note that although our benchmark scenario considers a mostly Bino $\tilde{\chi}_1^0$, we take into account how the relic density and proposed measurements depend on the gaugino mixing parameter μ. Our specific focus is placed on regions where the mass difference Δm between the stau ($\tilde{\tau}$) and the $\widetilde{\chi}_1^0$ is small ($\sim$ 5−25 GeV) [36], and where $\tilde{\tau}$ is produced through cascade decays of the lightest chargino $\widetilde{\chi}_1^{\pm}$ and the next-to-lightest neutralino $\widetilde{\chi}_2^0$ (with the colored SUSY sector decoupled) in processes such as $\widetilde{\chi}_1^+\widetilde{\chi}_1^- \rightarrow \tilde{\tau}\tilde{\tau}\nu_\tau\nu_\tau$, $\widetilde{\chi}_2^0\widetilde{\chi}_2^0 \rightarrow \tilde{\tau}\tilde{\tau}\tau\tau$, $\widetilde{\chi}_1^\pm\widetilde{\chi}_2^0 \rightarrow \tilde{\tau}\nu_\tau\tilde{\tau}\tau$ and $\widetilde{\chi}_1^\pm\widetilde{\chi}_1^0 \rightarrow \tilde{\tau}\nu_\tau\widetilde{\chi}_1^0$. This choice of mass spectra is driven by two facts: (1) compressed regions are difficult to probe at the LHC due to experimental constraints for events containing low p_T objects; (2) *a technique for the precision measurement of* $\Omega_{\widetilde{\chi}_1^0}h^2$ *at the LHC in this* $\tilde{\tau}-\widetilde{\chi}_1^0$ *CA region with a decoupled colored sector has not yet been developed*. In general, determining the mass and composition of $\widetilde{\chi}_1^0$ and measuring Δm in colored cascade searches (i.e. gluino and squark decays) requires reconstructing several kinematic endpoints simultaneously and in most cases requires one to assume model dependent correlations (e.g. grand unification to link the mass of the colored sector to the electroweak sector) [37]. Furthermore, the ATLAS and CMS experiments have pushed the limits of 1st and 2nd (3rd) generation squarks and gluinos to $\sim$ 2.1 TeV (1 TeV) [38–41], making $\widetilde{\chi}_1^0$ less accessible using colored SUSY searches. Therefore, in this paper we are motivated by the need for a less model-dependent methodology to deduce $\Omega_{\widetilde{\chi}_1^0}h^2$ in the difficult to probe compressed electroweak SUSY phase space, where the $\tilde{\tau}-\tilde{\chi}_1^0$ CA mechanism of the early Universe is important.

The targeted compressed scenario results in final states with multiple τ leptons with low-p_T visible decay products ($p_T \sim \frac{1}{3}\Delta m - \frac{1}{2}\Delta m$), making it difficult to reconstruct and identify more than one of them. We employ two search channels proposed as effective probes of the $\tilde{\tau}-\widetilde{\chi}_1^0$ CA region: (1) the invisible VBF channel with events where the visible τ decay products are too soft to reconstruct and identify, but where the two high-p_T forward jets boost the missing transverse energy (E_T^{miss}) to allow for an experimental trigger with low rate and sufficient background rejection [18,19,24]; (2) events with one high-p_T ISR jet and one τ_h (hadronic decay of the τ lepton), where the ISR jet boosts the system such that the transverse momentum of the τ_h is large enough to reconstruct and identify experimentally [25,26].

2. Samples and simulation

The signal and background samples are generated with MadGraph (v2.2.3) [42], interfaced with PYTHIA (v6.416) [43] to include quark/gluon fragmentation processes, and Delphes (v3.3.2) [44] to account for detector effects.

The first of two sets of signal samples considers pair production of electroweak SUSY particles with an associated ISR jet ($\widetilde{\chi}_l^{\pm,0}\widetilde{\chi}_k^{\pm,0}j$). The second set contains the same pairs of electroweak SUSY particles, except that production proceeds through the fusion of two SM vector bosons and results in two associated forward jets ($\widetilde{\chi}_l^{\pm,0}\widetilde{\chi}_k^{\pm,0}j_fj_f$). The signal scans consider $\widetilde{\chi}_1^\pm$ masses ranging from 100 to 400 GeV, Δm between 5 and 25 GeV, and $\widetilde{\chi}_1^0$ masses as low as 100 GeV. We select a benchmark reference point, not excluded by experiments, where $m(\tilde{\chi}_1^\pm)_{\rm benchmark} = 200$ GeV, $m(\tilde{\chi}_1^0)_{\rm benchmark} = 150$ GeV, and $\Delta m_{\rm benchmark} = 15$ GeV. In addition, we consider the $\widetilde{\chi}_1^\pm$ composition as mostly Wino. We note that we do take into account how the signal yields depend on the "ino" composition (e.g. a more Higgsino-like $\widetilde{\chi}_1^\pm$) by varying the gaugino mixing parameter μ. Background events are generated for the production of W, Z, top-quark pairs ($t\bar{t}$), and vector boson pairs (diboson) with up to four associated jets. Jet matching is performed with the MLM algorithm [45], which requires the optimization of two parameters: xqcut and qcut. The xqcut defines the minimal distance among partons at generation, while the qcut represents the minimum energy spread for a clustered jet in PYTHIA. The optimization of these two parameters, xqcut = 15 and qcut = 30–35 GeV, is performed using differential jet rate distributions from MADGRAPH, requiring a smooth transition between the curves for events with $n-1$ and n jets. Finally, a

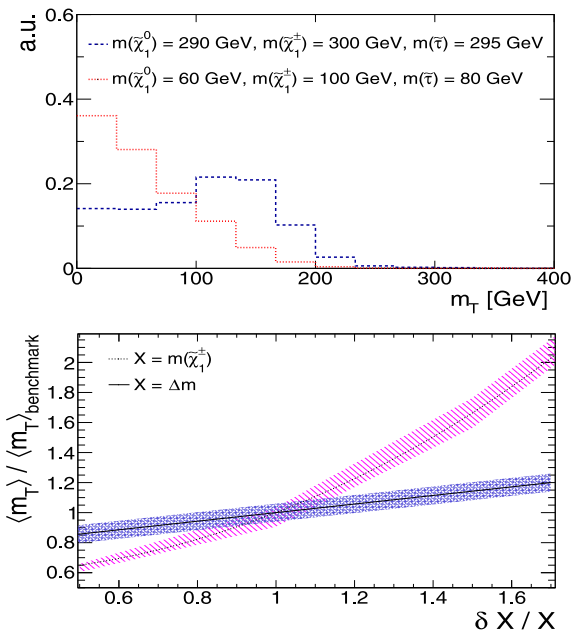

Fig. 1. The top panel shows the m_T distributions (normalized to unity) for two different $\tilde{\chi}_1^{\pm}$ masses. The lower panel displays $\langle m_T \rangle$ as a function of $m(\tilde{\chi}_1^{\pm})$ and Δm, keeping $m(\tilde{\chi}_1^0)$ constant.

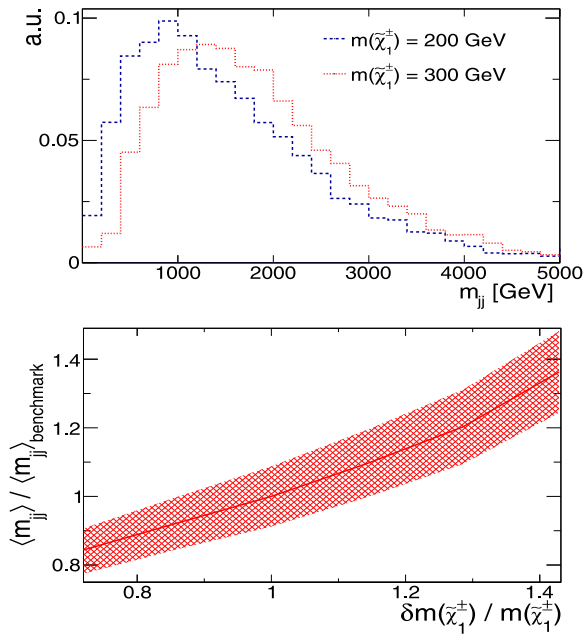

Fig. 2. The top panel shows the m_{jj} distributions (normalized to unity) for two different $\tilde{\chi}_1^{\pm}$ masses. The lower panel displays $\langle m_{jj} \rangle$ as a function of $m(\tilde{\chi}_1^{\pm})$, keeping Δm and $m(\tilde{\chi}_1^0)$ constant.

minimal event selection criteria, based on detector acceptance and experimental thresholds for particle identification, is applied at generation level, requiring leptons with $p_T(\ell) > 10$ GeV and $|\eta(\ell)| < 2.5$, while jets have a minimum p_T threshold of 20 GeV and $|\eta| < 5.0$.

3. Proposed methodology to measure $\Omega_{\tilde{\chi}_1^0} h^2$ at the LHC

For the VBF invisible search region, we follow suggested requirements in Refs. [18,19] and select simulated events with two forward highly-energetic jets ($p_T > 50$ GeV) in opposite hemispheres of the detector ($\eta_{jf_1} \times \eta_{jf_2} < 0$ and $|\Delta\eta(j_{f1}, j_{f2})| > 4.2$), and reconstructed dijet mass greater than 750 GeV. Furthermore, events containing b-tagged jets with $p_T > 20$ GeV or isolated leptons with $p_T > 10$ GeV (> 15 GeV for τ_h) and $|\eta| < 2.5$ are rejected.

The requirements for the ISR + $1\tau_h$ channel are similar to those of Ref. [25]. Simulated events are required to have one τ_h with $|\eta| < 2.3$ and p_T between 15 and 35 GeV. We veto events containing b-tagged jets or isolated leptons. The leading jet must have $p_T > 100$ GeV and $|\eta| < 2.5$. To ensure the ISR channel is exclusive to the VBF search sample, we veto events containing a second jet with $p_T > 50$ GeV, that combined with the leading jet could satisfy the VBF selection criteria.

As a cross-check, the results from Refs. [18,19,25] have been reproduced at a level of agreement $> 80\%$.

The VBF invisible channel uses the reconstructed mass between the two forward jet candidates, defined in Eq. (1), as the discriminating variable to look for an enhancement of events in the tails of the distribution that could suggest new physics. The ISR + $1\tau_h$ analysis uses the reconstructed transverse mass, defined in Eq. (2), between the τ_h and the E_T^{miss} from undetected $\tilde{\chi}_1^0$s.

$$m_{jfjf} = \sqrt{2p_T(j_{f1})p_T(j_{f2})cosh\Delta\eta(j_{f1}, j_{f2})} \quad (1)$$

$$m_T = \sqrt{2E_T^{miss}p_T(\tau_h)(1 - cos\Delta\phi(E_T^{miss}, \tau_h))} \quad (2)$$

Because of momentum and energy conservation, there is a correlation between $p_T(j)$, E_T^{miss}, and $p_T(\tau_h)$. In signal events, production of heavier electroweak SUSY particles requires jets with higher p_T. Therefore, the mean values of m_{jfjf} and m_T signal distributions ($\langle m_{jj} \rangle$ and $\langle m_T \rangle$) depend on $m(\tilde{\chi}_1^{\pm})$. Additionally, because $p_T(\tau_h)$ and E_T^{miss} depend on Δm as well as $m(\tilde{\chi}_1^0)$, the mean of the m_T distribution also depends on Δm and $m(\tilde{\chi}_1^0)$. The top panel of Fig. 1 shows the m_T distributions for two different signal points, while the lower panel of Fig. 1 displays $\langle m_T \rangle$ (normalized by $\langle m_T \rangle_{benchmark}$) as a function of $m(\tilde{\chi}_1^{\pm})$ and Δm, keeping $m(\tilde{\chi}_1^0)$ constant. The x-axis label $\delta X/X$ in the lower panel of Fig. 1 represents the relative variation of the $\tilde{\chi}_1^{\pm}$ (Δm) mass with respect to the benchmark value of $m(\tilde{\chi}_1^{\pm})_{\text{benchmark}} = 200$ GeV ($\Delta m = 15$ GeV). Similarly, the top panel of Fig. 2 shows the m_{jj} distributions for two different $\tilde{\chi}_1^{\pm}$ masses, while the lower panel displays $\langle m_{jj} \rangle$ (normalized by $\langle m_{jj} \rangle_{benchmark}$) as a function of the relative variation of $m(\tilde{\chi}_1^{\pm})$ with respect to $m(\tilde{\chi}_1^{\pm})_{\text{benchmark}}$, keeping $m(\tilde{\chi}_1^0)$ and Δm constant. The bands in Figs. 1 and 2 correspond to the statistical uncertainty on the mean values, calculated as the RMS of the distribution divided by the Poisson error on the signal yield assuming an integrated luminosity of $L_{int} = 50$ fb^{-1}. The values $\langle m_{jj} \rangle$ and $\langle m_T \rangle$ are parameterized as functions of the relevant masses: $\langle m_{jj} \rangle = f_{VBF}(m(\tilde{\chi}_1^{\pm}), m(\tilde{\chi}_1^0), \Delta m)$ and $\langle m_T \rangle = f_{ISR}(m(\tilde{\chi}_1^{\pm}), m(\tilde{\chi}_1^0), \Delta m)$.

Similarly, the signal yield in each channel is a function of $\tilde{\chi}_l^{\pm,0}\tilde{\chi}_k^{\pm,0}j_fj_f$ and $\tilde{\chi}_l^{\pm,0}\tilde{\chi}_k^{\pm,0}j$ production cross-sections. Therefore, the signal yields depend on $m(\tilde{\chi}_1^{\pm})$ and $m(\tilde{\chi}_1^0)$. The production cross-sections also depend on the "ino" composition of the neutralinos and charginos. The gaugino mixing is driven by the μ parameter: decreasing μ reduces the $\tilde{\chi}_1^0$ Bino composition by making the Higgsinos more important, and thus simultaneously decreases the Wino composition of $\tilde{\chi}_1^{\pm}/\tilde{\chi}_2^0$. Therefore, although our benchmark scenario considers the $\tilde{\chi}_1^{\pm}/\tilde{\chi}_2^0$ as mostly Wino, decreasing μ makes them more Higgsino-like. As noted previously, because $p_T(\tau_h)$ in the ISR channel depends on the mass difference between the $\tilde{\tau}$ and $\tilde{\chi}_1^0$, the number of signal events

also depend on Δm. Based on the above considerations, the signal yields in the VBF invisible and ISR + soft-τ_h channels are parameterized as follows: $N_{VBF} = g_{VBF}(m(\tilde{\chi}_1^{\pm}), m(\tilde{\chi}_1^0), \Delta m, \mu)$ and $N_{ISR} = g_{ISR}(m(\tilde{\chi}_1^{\pm}), m(\tilde{\chi}_1^0), \Delta m, \mu)$.

Therefore, by combining the VBF invisible and ISR $+1\tau_h$ search channels at ATLAS/CMS, there are enough independent observables to extract the measurement of all the relevant SUSY particle masses. If the CMS and ATLAS experiments observe an excess of events in the VBF invisible and ISR + soft-τ_h channels, the relevant particle masses, gaugino mixing parameter μ, and their uncertainties can be deduced from the "bumps" in the m_{jj} and m_T distributions. This is accomplished by using the m_T and m_{jj} distributions to perform a shape based determination of the signal parameters with the test statistic defined from a profile binned likelihood ratio approach via the RooFit toolkit [46]. For each of the two channels, the parameters of interest are the signal strength factors r_i and template m_T or m_{jj} shapes s_i. The parameter r_i represents the weight on the number of predicted signal events for assumed model i (model i is one given signal sample or set of SUSY parameters $m(\tilde{\chi}_1^{\pm})$, $m(\tilde{\chi}_1^0)$, Δm, and μ). This weight factor r_i is defined such that $r_i = 0$ corresponds to the background-only hypothesis and $r_i = 1$ corresponds to the signal prediction in model i in addition to the background. The profile likelihood ratio test statistic extracts the information of the best fit signal strength and shape from a full likelihood fit to the data. The likelihood function also includes all the parameters that describe the systematic uncertainties and their correlations, and are incorporated using nuisance parameters. For the VBF invisible channel, we use the VBF SUSY searches at CMS as a guideline for determining the dominant systematic effects. We assume a 24% uncertainty on the SM backgrounds due to the measurement of the VBF selection efficiency, and a 20% uncertainty in the signal yields arising from the calibration of forward jets [17,19]. These uncertainties are treated fully correlated between signal and background. For the ISR + $1\tau_h$ channel, we follow the prescription from Ref. [25] and assume 10% systematic uncertainty on both background and signal, considering them to be uncorrelated. The 10% systematic uncertainty contains dominant contributions from the uncertainty on τ_h identification (6%), E_T^{miss} trigger efficiency (1%), modeling of ISR (5%), pileup effects, and the uncertainty on transfer factors used to estimate the backgrounds [47–54]. In the actual experimental analysis this likelihood fit is performed on the observed data using a signal plus background hypothesis to extract the best fit r_i and s_i. For the purpose of this paper, we simulate the observed experimental outcome by creating 10^8 toy datasets assuming the presence of background and signal. For each toy dataset we derive the best fit r_i and s_i, resulting in the extraction of the mean values of the m_{jj} and m_T signal distributions, the best fit signal yields, and subsequently inverting the four functions $\langle m_{jj} \rangle = f_{VBF}(m(\tilde{\chi}_1^{\pm}), m(\tilde{\chi}_1^0), \Delta m), N_{VBF} = g_{VBF}(m(\tilde{\chi}_1^{\pm}), m(\tilde{\chi}_1^0), \Delta m, \mu), \langle m_T \rangle = f_{ISR}(m(\tilde{\chi}_1^{\pm}), m(\tilde{\chi}_1^0), \Delta m)$, and N_{ISR}=$g_{ISR}(m(\tilde{\chi}_1^{\pm}), m(\tilde{\chi}_1^0), \Delta m, \mu)$ to extract measurements of the particle masses and mixing parameter. Each toy dataset gives a different best fit r_i and s_i, which determines the uncertainty on the measured parameters. With 500 fb^{-1} of 13 TeV pp data from the LHC, we obtain (in GeV) $m(\tilde{\chi}_1^{\pm}) = 200 \pm 6.2$, $m(\tilde{\chi}_1^0) = 150 \pm 7.8$, $\Delta m = 15.0 \pm 1.7$, and $\mu = 500 \pm 42.0$ for our benchmark scenario.

We note that the determination of small Δm would confirm that we are indeed in the $\tilde{\tau} - \tilde{\chi}_1^0$ CA region. It is also important to note that the precision measurements of the sparticle masses is critical not only for the accurate calculation of $\Omega_{\tilde{\chi}_1^0} h^2$, but also for purposes beyond the cosmology connection. For example, the precise measurement of the $\tilde{\tau}$ mass has relevant effects on precision electroweak measurements such as higher-order contributions to the W mass and the muon anomalous magnetic moment [55]. Table 1 shows the values and associated errors for the $m(\tilde{\chi}_1^{\pm})$, $m(\tilde{\chi}_1^0)$, Δm, and $m(\tilde{\tau})$ parameters of the two different benchmark points used in the study, assuming two different integrated luminosity values at the LHC. Table 2 shows the corresponding results for a scenario where the $\tilde{\chi}_1^{\pm}/\tilde{\chi}_2^0$ composition is mostly Higgsino. The smaller Higgsino cross sections result in larger uncertainties compared to the Wino benchmark scenarios.

Table 1
Values and corresponding errors for the $m(\tilde{\chi}_1^{\pm})$, $m(\tilde{\chi}_1^0)$, Δm, and μ parameters, for the two Wino benchmark signal points (P1 and P2) used in the study. The results are reported for two different expected luminosity scenarios at the LHC: 500 fb^{-1} and 3000 fb^{-1}.

x [GeV]	P1 [500 (3000) fb^{-1}]	P2 [500 (3000) fb^{-1}]
$m(\tilde{\chi}_1^{\pm})$	200 ± 6.2 (200 ± 2.4)	300 ± 13.8 (300 ± 5.6)
$m(\tilde{\chi}_1^0)$	150 ± 7.8 (150 ± 3.2)	250 ± 19.5 (250 ± 8.0)
Δm	15.0 ± 1.7 (15.0 ± 0.7)	15.0 ± 2.5 (15.0 ± 1.0)
$m(\tilde{\tau})$	175 ± 8.4 (175 ± 3.4)	275 ± 20.0 (275 ± 8.1)

Table 2
Values and corresponding errors for the $m(\tilde{\chi}_1^{\pm})$, $m(\tilde{\chi}_1^0)$, Δm, and μ parameters, for two benchmark signal points (P1 and P2), considering the $\tilde{\chi}_1^{\pm}/\tilde{\chi}_2^0$ composition as mostly Higgsino. The results are reported for two different expected luminosity scenarios at the LHC: 500 fb^{-1} and 3000 fb^{-1}.

x [GeV]	P1 [500 (3000) fb^{-1}]	P2 [500 (3000) fb^{-1}]
$m(\tilde{\chi}_1^{\pm})$	200 ± 8.9 (200 ± 3.6)	300 ± 20.2 (300 ± 8.2)
$m(\tilde{\chi}_1^0)$	150 ± 11.3 (150 ± 4.6)	250 ± 28.5 (250 ± 11.6)
Δm	15.0 ± 2.4 (15.0 ± 1.0)	15.0 ± 3.7 (15.0 ± 1.5)
$m(\tilde{\tau})$	175 ± 12.3 (175 ± 5.0)	275 ± 29.1 (275 ± 11.9)

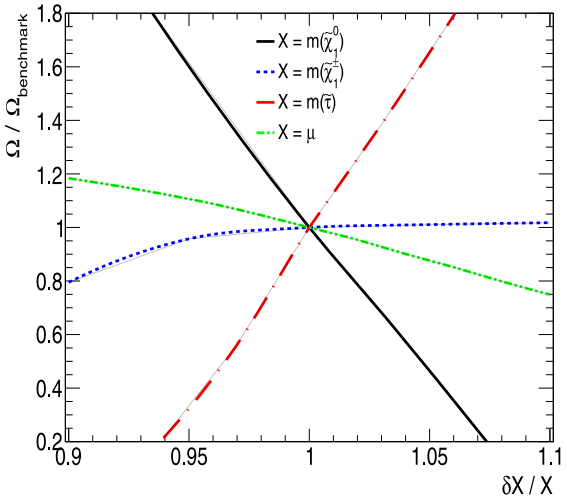

Fig. 3. $\Omega_{\tilde{\chi}_1^0} h^2$ as a function of $m(\tilde{\chi}_1^{\pm})$, $m(\tilde{\chi}_1^0)$, Δm, and μ. For a given curve, all other parameters are fixed.

After measuring the sparticle masses and gaugino mixing parameter, we calculate $\Omega_{\tilde{\chi}_1^0} h^2$ using micrOMEGAs version 4.3 [56]. The relic density depends on the "ino" composition of $\tilde{\chi}_1^0$, $m(\tilde{\chi}_1^0)$, and Δm (since $\langle \sigma v \rangle_{CA}$ depends on the Boltzmann factor $e^{-\Delta m/T}$ in the relic density formula). Fig. 3 shows $\Omega_{\tilde{\chi}_1^0} h^2$ as a function of $m(\tilde{\chi}_1^{\pm})$, $m(\tilde{\chi}_1^0)$, Δm, and μ. For a given curve, all other parameters are fixed. For example, the $\Omega_{\tilde{\chi}_1^0} h^2$ vs. Δm curve is obtained by fixing $m(\tilde{\chi}_1^{\pm})$, $m(\tilde{\chi}_1^0)$, and μ.

Since $\Omega_{\tilde{\chi}_1^0} h^2$ is inversely related to the coannihilation cross-section $\langle \sigma v \rangle_{CA} \sim e^{-\Delta m/T}$, then $\Omega_{\tilde{\chi}_1^0} h^2 \sim e^{\Delta m/T}$. Thus as $\Delta m/T$ increases in Fig. 3, so does $\Omega_{\tilde{\chi}_1^0} h^2$. Furthermore, since decreasing

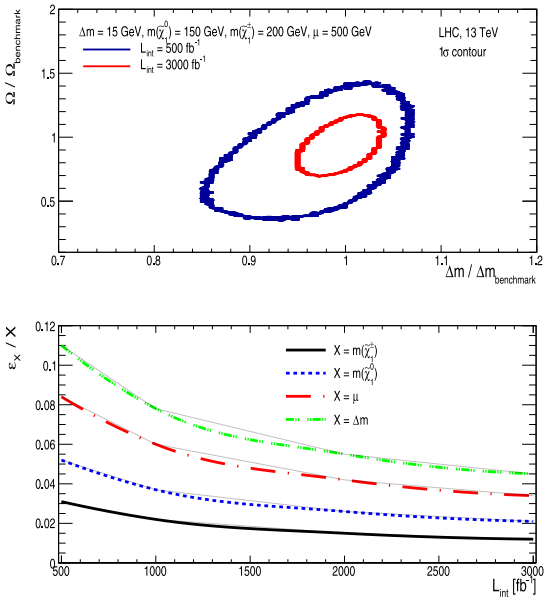

Fig. 4. Top panel: $\Omega_{\tilde{\chi}_1^0}h^2-\Delta m$ contour plot (1 standard deviation). Bottom panel: sparticle mass and μ measurement uncertainties vs. integrated luminosity, for the benchmark point used (Δm = 15 GeV, $m(\tilde{\chi}_1^0)$ = 150 GeV, $m(\tilde{\chi}_1^{\pm})$ = 200 GeV, and μ = 500 GeV).

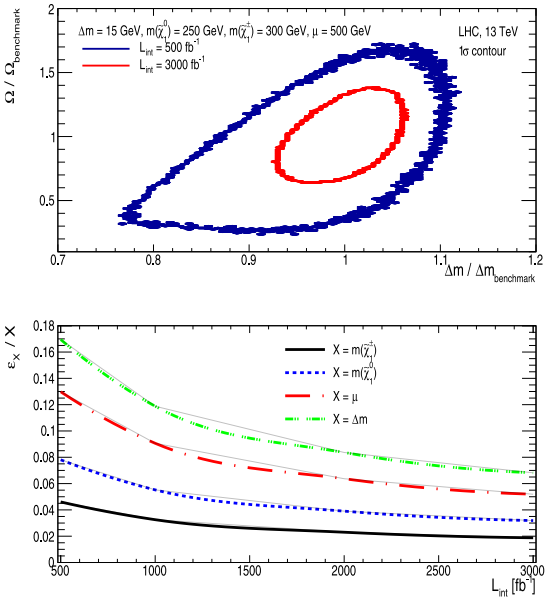

Fig. 5. Top panel: $\Omega_{\tilde{\chi}_1^0}h^2-\Delta m$ contour plot (1 standard deviation). Bottom panel: sparticle mass and μ measurement uncertainties vs. integrated luminosity, for a signal point with Δm = 15 GeV, $m(\tilde{\chi}_1^0)$ = 250 GeV, $m(\tilde{\chi}_1^{\pm})$ = 300 GeV, and μ = 500 GeV.

μ decreases the Bino and Wino compositions of $\tilde{\chi}_1^0$, the annihilation cross-section $\langle\sigma v\rangle$ also decreases, which in turn increases $\Omega_{\tilde{\chi}_1^0}h^2$. Finally, as $m(\tilde{\chi}_1^0)$ increases, it is less likely that SM particles had enough thermal kinetic energy in the early universe to create heavier DM particles. Therefore, $\Omega_{\tilde{\chi}_1^0}h^2$ in Fig. 3 decreases with $m(\tilde{\chi}_1^0)$.

Since the DM relic density can be parameterized as $\Omega_{\tilde{\chi}_1^0}h^2 = h(m(\tilde{\chi}_1^{\pm}), m(\tilde{\chi}_1^0), \Delta m, \mu)$, by combining the measurements of the three sparticle masses and gaugino mixing parameter, the DM relic density can be deduced. The top panel of Fig. 4 shows contour plots of the uncertainty (one standard deviation) in the $\Omega_{\tilde{\chi}_1^0}h^2-\Delta m$ plane (normalized by $\Omega_{\tilde{\chi}_1^0}h^2$ and Δm central values for the benchmark point). The uncertainty on $\Omega_{\tilde{\chi}_1^0}h^2$ is 25 (45)% at 3000 (500) fb^{-1}. Fig. 4 (bottom panel) also shows how well the sparticle masses and gaugino mixing can be measured as a function of integrated luminosity. Note the dominant contribution to the uncertainty on $\Omega_{\tilde{\chi}_1^0}h^2$ is from the measurement of Δm (4.5% at L_{int} = 3000 fb^{-1}). To show how these measurements change with increasing $\tilde{\chi}_1^{\pm}/\tilde{\chi}_2^0$ masses, Fig. 5 shows a similar $\Omega_{\tilde{\chi}_1^0}h^2-\Delta m$ contour plot of the uncertainty for a different signal point: Δm = 15 GeV, $m(\tilde{\chi}_1^0)$ = 250 GeV, $m(\tilde{\chi}_1^{\pm})$ = 300 GeV, and μ = 500 GeV. The uncertainties on $\Omega_{\tilde{\chi}_1^0}h^2$ and Δm are 37% and 7% at 3000 fb^{-1}, respectively. The uncertainties are larger with respect to the original benchmark point, due to smaller cross sections and thus smaller signal yields.

4. Discussion

In conclusion, a technique has been developed for the measurement of $\Omega_{\tilde{\chi}_1^0}h^2$ in the $\tilde{\tau}-\tilde{\chi}_1^0$ CA region, using observables from the VBF invisible and ISR + $1\tau_h$ searches for compressed SUSY at the LHC. The methodology established in this paper is agnostic to the mass scale of the colored SUSY sector. This approach allows for the determination of $\Omega_{\tilde{\chi}_1^0}h^2$ at the LHC for any model where $\tilde{\tau}-\tilde{\chi}_1^0$ CA is an important DM reduction mechanism in the early Universe. $\Omega_{\tilde{\chi}_1^0}h^2$ can be measured with an uncertainty of 25% (45%) with 3000 (500) fb^{-1} of 13 TeV proton–proton data. This is a critical link between particle physics and cosmology, providing valuable information to help determine whether the DM we observe gravitationally is indeed made out by $\tilde{\chi}_1^0$s created in the early Universe. On the other hand, if $\tilde{\chi}_1^0$s are discovered with the VBF/ISR analyses and the deduced relic density is not consistent with astronomy, this could lead to a reconsideration of our assumptions of the evolution of the Universe. In either case, a discovery at the LHC with the VBF/ISR analyses and the subsequent determination of the $\tilde{\chi}_1^0$ relic density has the potential to break significant ground on the identity of DM, one of the most relevant questions in science.

Declaration of competing interest

The authors declare that they have no known competing financial interests or personal relationships that could have appeared to influence the work reported in this paper.

Acknowledgments

We thank the constant and enduring financial support received for this project from the faculty of science at Universidad de los Andes (Bogotá, Colombia), and by the Foundation for the promotion of research and technology of Bank of the Republic of Colombia under project number 4262, the administrative department of science, technology and innovation of Colombia (COLCIENCIAS), the Physics & Astronomy department at Vanderbilt University, USA and the US National Science Foundation. This work is supported in part by NSF, USA Award PHY-1806612.

References

[1] G. Hinshaw, et al., [WMAP Collaboration], Nine-year wilkinson microwave anisotropy probe (WMAP) observations: Cosmological parameter results, Astrophys. J. Suppl. 208 (2013) 19, http://dx.doi.org/10.1088/0067-0049/208/2/19, [arXiv:1212.5226 [astro-ph.CO]].

[2] N. Aghanim, et al., [Planck Collaboration], Planck 2018 results. VI. Cosmological parameters, arXiv:1807.06209 [astro-ph.CO].

[3] G. Bertone, D. Hooper, J. Silk, Particle dark matter: Evidence, candidates and constraints, Phys. Rep. 405 (2005) 279–390, http://dx.doi.org/10.1016/j.physrep.2004.08.031, [arXiv:hep-ph/0404175v2 [hep-ph]].

[4] G. Aad, et al., [ATLAS Collaboration], The ATLAS experiment at the CERN large hadron collider, JINST 3 (2008) S08003, http://dx.doi.org/10.1088/1748-0221/3/08/S08003.

[5] S. Chatrchyan, et al., [CMS Collaboration], The CMS experiment at the CERN LHC, JINST 3 (2008) S08004, http://dx.doi.org/10.1088/1748-0221/3/08/S08004.

[6] G. Aad, et al., [ATLAS Collaboration], Observation of a new particle in the search for the Standard Model Higgs boson with the ATLAS detector at the LHC, Phys. Lett. B 716 (1) (2012) 1–29, http://dx.doi.org/10.1016/j.physletb.2012.08.020, [arXiv:1207.7214 [hep-ex]].

[7] V. Khachatryan, et al., [CMS Collaboration], Observation of a new boson at a mass of 125 GeV with the CMS experiment at the LHC, Phys. Lett. B 716 (1) (2012) 30–61, http://dx.doi.org/10.1016/j.physletb.2012.08.021, [arXiv:1207.7235 [hep-ex]].

[8] N. Du, et al., [ADMX Collaboration], A search for invisible axion dark matter with the axion dark matter experiment, Phys. Rev. Lett. 120 (15) (2018) 151301, http://dx.doi.org/10.1103/PhysRevLett.120.151301, [arXiv:1804.05750 [hep-ex]].

[9] C.M. Ho, R.J. Scherrer, Anapole dark matter, Phys. Lett. B 722 (2013) 341, http://dx.doi.org/10.1016/j.physletb.2013.04.039, [arXiv:1211.0503 [hep-ph]].

[10] P. Ramond, Dual theory for free fermions, Phys. Rev. D 3 (1971) 2415, http://dx.doi.org/10.1103/PhysRevD.3.2415.

[11] S. Ferrara, B. Zumino, Supergauge invariant Yang–Mills theories, Nuclear Phys. B 79 (1974) 413, http://dx.doi.org/10.1016/0550-3213(74)90559-8.

[12] J. Wess, B. Zumino, Supergauge transformations in four dimensions, Nuclear Phys. B 70 (1974) 39, http://dx.doi.org/10.1016/0550-3213(74)90355-1.

[13] A.H. Chamseddine, R.L. Arnowitt, P. Nath, Locally supersymmetric grand unification, Phys. Rev. Lett. 49 (1982) 970, http://dx.doi.org/10.1103/PhysRevLett.49.970.

[14] R. Barbieri, S. Ferrara, C.A. Savoy, Gauge models with spontaneously broken local 534 supersymmetry, Phys. Lett. B 119 (1982) 343, http://dx.doi.org/10.1016/0370-2693(82)90685-2.

[15] S.P. Martin, A supersymmetry primer, Adv. Ser. Direct. High Energy Phys. 21 (2010) 1; Adv. Ser. Direct. High Energy Phys. 18 (1998) 1, http://dx.doi.org/10.1142/9789812839657_0001, http://dx.doi.org/10.1142/9789814307505_0001 [hep-ph/9709356].

[16] B. Dutta, A. Gurrola, W. Johns, T. Kamon, P. Sheldon, K. Sinha, Vector boson fusion processes as a probe of supersymmetric electroweak sectors at the LHC, Phys. Rev. D 87 (3) (2013) 035029, http://dx.doi.org/10.1103/PhysRevD.87.035029, [arXiv:1210.0964 [hep-ph]].

[17] V. Khachatryan, et al., [CMS Collaboration], Search for supersymmetry in the vector-boson fusion topology in proton–proton collisions at $\sqrt{s}$ = 8TeV, J. High Energy Phys. 1511 (2015) 189, http://dx.doi.org/10.1007/JHEP11(2015)189, [arXiv:1508.07628 [hep-ex]].

[18] A. Delannoy, et al., Probing dark matter at the LHC using vector boson fusion processes, Phys. Rev. Lett. 111 (2013) 061801, http://dx.doi.org/10.1103/PhysRevLett.111.061801, [arXiv:1304.7779 [hep-ph]].

[19] V. Khachatryan, et al., [CMS Collaboration], Search for dark matter and supersymmetry with a compressed mass spectrum in the vector boson fusion topology in proton-proton collisions at $\sqrt{s} = 8$ tev, Phys. Rev. Lett. 118 (2) (2017) 021802, http://dx.doi.org/10.1103/PhysRevLett.118.021802, [arXiv:1605.09305 [hep-ex]].

[20] B. Dutta, T. Ghosh, A. Gurrola, W. Johns, T. Kamon, P. Sheldon, K. Sinha, S. Wu, Probing compressed sleptons at the LHC using vector boson fusion processes, Phys. Rev. D 91 (2015) 055025, http://dx.doi.org/10.1103/PhysRevD.91.055025, [arXiv:1411.6043 [hep-ph]].

[21] B. Dutta, W. Flanagan, A. Gurrola, W. Johns, T. Kamon, P. Sheldon, K. Sinha, K. Wang, S. Wu, Probing compressed top squarks at the LHC at 14 TeV, Phys. Rev. D 90 (2014) 095022, http://dx.doi.org/10.1103/PhysRevD.90.095022, [arXiv:1312.1348 [hep-ph]].

[22] B. Dutta, et al., Probing compressed bottom squarks with boosted jets and shape analysis, Phys. Rev. D 92 (2015) 095009, http://dx.doi.org/10.1103/PhysRevD.92.095009, [arXiv:1507.01001 [hep-ph]].

[23] A. Flórez, A. Gurrola, W. Johns, J. Maruri, P. Sheldon, K. Sinha, S.R. Starko, Anapole dark matter via vector boson fusion processes at the LHC, Phys. Rev. D 100 (1) (2019) 016017, http://dx.doi.org/10.1103/PhysRevD.100.016017, [arXiv:1902.01488 [hep-ph]].

[24] A.M. Sirunyan, et al., [CMS Collaboration], Search for supersymmetry with a compressed mass spectrum in the vector boson fusion topology with 1-lepton and 0-lepton final states in proton–proton collisions at $\sqrt{s}$ = 13 TeV, J. High Energy Phys. 1908 (2019) 150, http://dx.doi.org/10.1007/JHEP08(2019)150, [arXiv:1905.13059 [hep-ex]].

[25] A. Flórez, L. Bravo, A. Gurrola, C. Ávila, M. Segura, P. Sheldon, W. Johns, Probing the stau-neutralino coannihilation region at the LHC with a soft tau lepton and a jet from initial state radiation, Phys. Rev. D 94 (7) (2016) 073007, http://dx.doi.org/10.1103/PhysRevD.94.073007, [arXiv:1606.08878 [hep-ph]].

[26] A.M. Sirunyan, et al., [CMS Collaboration], Search for supersymmetry with a compressed mass spectrum in events with a soft τ lepton, a highly energetic jet, and large missing transverse momentum in proton–proton collisions at $\sqrt{s} = 13$ TeV, arXiv:1910.01185 [hep-ex].

[27] A.M. Sirunyan, et al., [CMS Collaboration], Search for new physics in final states with an energetic jet or a hadronically decaying W or Z boson and transverse momentum imbalance at $\sqrt{s} = 13TeV$, Phys. Rev. D 97 (9) (2018) 092005, http://dx.doi.org/10.1103/PhysRevD.97.092005, [arXiv:1712.02345 [hep-ex]].

[28] V. Khachatryan, et al., [CMS Collaboration], Search for dark matter, extra dimensions, and unparticles in monojet events in proton–proton collisions at $\sqrt{s} = 8$TeV, Eur. Phys. J. C 75 (5) (2015) 235, http://dx.doi.org/10.1140/epjc/s10052-015-3451-4, [arXiv:1408.3583 [hep-ex]].

[29] M. Aaboud, et al., [ATLAS Collaboration], Search for dark matter and other new phenomena in events with an energetic jet and large missing transverse momentum using the ATLAS detector, J. High Energy Phys. 1801 (2018) 126, http://dx.doi.org/10.1007/JHEP01(2018)126, [arXiv:1711.03301 [hep-ex]].

[30] A. Flórez, A. Gurrola, W. Johns, Y.D. Oh, P. Sheldon, D. Teague, T. Weiler, Searching for new heavy neutral gauge bosons using vector boson fusion processes at the LHC, Phys. Lett. B 767 (2017) 126, http://dx.doi.org/10.1016/j.physletb.2017.01.062, [arXiv:1609.09765 [hep-ph]].

[31] A. Flórez, K. Gui, A. Gurrola, C. Patio, D. Restrepo, Expanding the reach of heavy neutrino searches at the LHC, Phys. Lett. B 778 (2018) 94, http://dx.doi.org/10.1016/j.physletb.2018.01.009, [arXiv:1708.03007 [hep-ph]].

[32] A. Flórez, Y. Guo, A. Gurrola, W. Johns, O. Ray, P. Sheldon, S. Starko, Probing heavy spin-2 bosons with $\gamma\gamma$ final states from vector boson fusion processes at the LHC, Phys. Rev. D 99 (3) (2019) 035034, http://dx.doi.org/10.1103/PhysRevD.99.035034, [arXiv:1812.06824 [hep-ph]].

[33] R.H. Brandenberger, Introduction to early universe cosmology, PoS ICFI 2010 (2010) 001, [arXiv:1103.2271 [astro-ph.CO]].

[34] M.J. Baker, et al., The coannihilation codex, J. High Energy Phys. 1512 (2015) 120, http://dx.doi.org/10.1007/JHEP12(2015)120, [arXiv:1510.03434 [hep-ph]].

[35] K. Griest, D. Seckel, Three exceptions in the calculation of relic abundances, Phys. Rev. D 43 (1991) 3191, http://dx.doi.org/10.1103/PhysRevD.43.3191.

[36] A. Aboubrahim, P. Nath, A.B. Spisak, Stau. Coannihilation, Stau coannihilation compressed spectrum and SUSY discovery at the LHC, Phys. Rev. D 95 (2017) 115030, http://dx.doi.org/10.1103/PhysRevD.95.115030, [arXiv:1704.04669 [hep-ph]].

[37] R.L. Arnowitt, B. Dutta, A. Gurrola, T. Kamon, A. Krislock, D. Toback, Determining the dark matter relic density in the mSUGRA (X0(1))- tau coannhiliation region at the LHC, Phys. Rev. Lett. 100 (2008) 231802, http://dx.doi.org/10.1103/PhysRevLett.100.231802, [arXiv:0802.2968 [hep-ph]].

[38] V. Khachatryan, et al., [CMS Collaboration], Search for new physics in the multijet and missing transverse momentum final state in proton–proton collisions at $\sqrt{s} = 8$TeV, J. High Energy Phys. 06 (2014) 055, http://dx.doi.org/10.1007/JHEP06(2014)055, [arXiv:1402.4770 [hep-ex]].

[39] V. Khachatryan, et al., [CMS Collaboration], Search for supersymmetry in multijet events with missing transverse momentum in proton–proton collisions at 13TeV, Phys. Rev. D 96 (2017) 032003, http://dx.doi.org/10.1103/PhysRevD.96.032003.

[40] M. Aaboud, et al., [ATLAS Collaboration], Search for new phenomena using the invariant mass distribution of same-flavour opposite-sign dilepton pairs in events with missing transverse momentum in $\sqrt{s} = 13$ TeV pp collisions with the ATLAS detector, Eur. Phys. J. C 78 (8) (2018) 625, http://dx.doi.org/10.1140/epjc/s10052-018-6081-9, [arXiv:1805.11381 [hep-ex]].

[41] M. Aaboud, et al., [ATLAS Collaboration], Search for heavy charged long-lived particles in the ATLAS detector in 36.1 fb^{-1} of proton–proton collision data at $\sqrt{s} = 13$TeV, Phys. Rev. D 99 (9) (2019) 092007, http://dx.doi.org/10.1103/PhysRevD.99.092007, [arXiv:1902.01636 [hep-ex]].

[42] J. Alwall, et al., The automated computation of tree-level and next-to-leading order differential cross sections, and their matching to parton shower simulations, J. High Energy Phys. 1407 (2014) 079, http://dx.doi.org/10.1007/JHEP07(2014)079, [arXiv:1405.0301 [hep-ph]].

[43] T. Sjostrand, S. Mrenna, P.Z. Skands, PYTHIA 6.4 physics and manual, J. High Energy Phys. 0605 (2006) 026, http://dx.doi.org/10.1088/1126-6708/2006/05/026, [arXiv:0603175 [hep-ph]].

[44] J. de Favereau, et al., [DELPHES 3 Collaboration], DELPHES 3, A modular framework for fast simulation of a generic collider experiment, J. High Energy Phys. 1402 (2014) 057, http://dx.doi.org/10.1007/JHEP02(2014)057.

[45] J. Alwall, et al., Comparative study of various algorithms for the merging of parton showers and matrix elements in hadronic collisions, Eur. Phys. J. C 53 (2008) 473, http://dx.doi.org/10.1140/epjc/s10052-007-0490-5, [arXiv:0706.2569 [hep-ex]].

[46] L. Moneta, K. Belasco, K.S. Cranmer, S. Kreiss, A. Lazzaro, et al., The RooStats project, PoS ACAT 2010 (2010) 057, [arXiv:1009.1003 [physics.data-an]].

[47] V. Khachatryan, et al., [CMS Collaboration], Search for heavy resonances decaying to tau lepton pairs in proton–proton collisions at $\sqrt{s}$ = 13TeV, J. High Energy Phys. 1702 (2017) 048, http://dx.doi.org/10.1007/JHEP02(2017)048, [arXiv:1611.06594 [hep-ex]].

[48] V. Khachatryan, et al., [CMS Collaboration], Search for pair production of third-generation scalar leptoquarks and top squarks in proton?proton collisions at $\sqrt{s} = 8$ TeV, Phys. Lett. B 739 (2014) 229, http://dx.doi.org/10.1016/j.physletb.2014.10.063, [arXiv:1408.0806 [hep-ex]].

[49] V. Khachatryan, et al., [CMS Collaboration], Search for heavy neutrinos or third-generation leptoquarks in final states with two hadronically decaying τ leptons and two jets in proton–proton collisions at $\sqrt{s} = 13$TeV, J. High Energy Phys. 1703 (2017) 077, http://dx.doi.org/10.1007/JHEP03(2017)077, [arXiv:1612.01190 [hep-ex]].

[50] A.M. Sirunyan, et al., [CMS Collaboration], Search for heavy neutrinos and third-generation leptoquarks in hadronic states of two τ leptons and two jets in proton–proton collisions at $\sqrt{s} = 13$ TeV, J. High Energy Phys. 1903 (2019) 170, http://dx.doi.org/10.1007/JHEP03(2019)170, [arXiv:1811.00806 [hep-ex]].

[51] A.M. Sirunyan, et al., [CMS Collaboration], Search for third-generation scalar leptoquarks and heavy right-handed neutrinos in final states with two tau leptons and two jets in proton–proton collisions at $\sqrt{s}$ = 13TeV, J. High Energy Phys. 1707 (2017) 121, http://dx.doi.org/10.1007/JHEP07(2017)121, [arXiv:1703.03995 [hep-ex]].

[52] S. Chatrchyan, et al., [CMS Collaboration], Search for physics beyond the standard model in events with τ leptons, jets, and large transverse momentum imbalance in pp collisions at $\sqrt{s} = 7$ TeV, Eur. Phys. J. C 73 (2013) 2493, http://dx.doi.org/10.1140/epjc/s10052-013-2493-8, [arXiv:1301.3792 [hep-ex]].

[53] S. Chatrchyan, et al., [CMS Collaboration], Search for pair production of third-generation leptoquarks and top squarks in pp collisions at $\sqrt{s}$ = 7TeV, Phys. Rev. Lett. 110 (8) (2013) 081801, http://dx.doi.org/10.1103/PhysRevLett.110.081801, [arXiv:1210.5629 [hep-ex]].

[54] S. Chatrchyan, et al., [CMS Collaboration], Search for high-mass resonances decaying into τ-lepton pairs in pp collisions at $\sqrt{s}$ = 7TeV, Phys. Lett. B 716 (2012) 82, http://dx.doi.org/10.1016/j.physletb.2012.07.062, [arXiv:1206.1725 [hep-ex]].

[55] M. Carena, S. Gori, N.R. Shah, C.E.M. Wagner, L.T. Wang, Light stau phenomenology and the higgs $\gamma\gamma$ rate, J. High Energy Phys. 1207 (2012) 175, http://dx.doi.org/10.1007/JHEP07(2012)175, [arXiv:1205.5842 [hep-ph]].

[56] D. Barducci, G. Belanger, J. Bernon, F. Boudjema, J. Da Silva, S. Kraml, U. Laa, A. Pukhov, Collider limits on new physics within micrOMEGAs4.3, [arXiv:1606.03834 [hep-ph]].